Design and Analysis of a Thermally Insulating and Heating Scheme for Piezoelectric Stack Actuators Used in the Cryogenic Environment

ZHANG Lei[1], *XIAO Yan*[2], *JIANG Yongping*[3], *CHEN Mingxuan*[4], *SHEN Xing*[1*]

1. State Key Laboratory of Mechanics and Control of Mechanical Structures，Nanjing University of Aeronautics and Astronautics，Nanjing 210016，P. R. China；
2. Shanghai Institute of Satellite Engineering，Shanghai 200240，P. R. China；
3. Aircraft Strength Research Institute of China，Xi'an 710065，P. R. China；
4. Nanjing Chenguang Group Co.,Ltd.，Nanjing 210006，P. R. China

Abstract: In cryogenic wind tunnel tests，piezoelectric stacks are adopted to realize the vibration control of the cantilever sting. However，the free stroke and blocking force of the piezoelectric stack would decrease dramatically as the temperature decreases. This paper proposes a convenient and effective warming structure for the piezoelectric stack，which could keep it working at operating temperatures when the ambient temperature drops. The piezoelectric stack actuator is wrapped with the heating film，and this resulting assembly is then wrapped with the aerogel material for thermal insulation. Both ends of the piezoelectric stack actuator make direct contact with the payload structure. Both one-dimensional and two-dimensional theoretical analyses of the heating conduction problem of the piezoelectric stack actuator are conducted. These analyses results are compared with those of the finite element simulation analysis. The finite element method results show a good consistency with the two-dimensional theoretical results，and a slight deviation of only 0.91 K is observed，indicating its potential for protecting piezoelectric stacks at low temperatures.

Key words： piezoelectric stack actuator；cryogenic environment；heating structure；one-dimensional heat conduction；two-dimensional heat conduction

0　Introduction

Aerodynamic parameters such as lift and drag can be obtained by wind tunnel test by simulating the aircraft's aerodynamic-flow field in flight，which has great significance in the aircraft design and evaluation. During the wind tunnel test，the cantilever sting is used to support the test model. However，harmful vibration will occur because the natural frequencies of the slender sting are easy to be coupled with the incoming turbulence，which will directly affect the test accuracy. The magnitude of damping changes is higher for high Reynolds number tests resulting in net negative sting damping and divergent oscillations. In order to solve this problem，the piezoelectric stack is used for active vibration control of the cantilever sting[1-5]. The high Reynolds number tests are conducted with cryogenic airflow，whose temperature could dramatically drop to －150 ℃. However，such a low temperature will make a significantly negative impact on the piezoelectric stack，resulting in reducing the performance of the active vibration suppression. Sherrit et al[6-7] investigated the temperature dependence of the piezoelectric stacks material properties from －180 ℃ to 200 ℃. Taylor et al.[8] designed a test facility to achieve pre-

cise measurements of the PZT stack actuator constant (d33) and proved that the nominal value of the piezoelectric constant was reduced to approximately one-third of its nominal room temperature value at 40 K. Specifically, the full range displacement and driving force of piezoelectric stack decrease dramatically in a monotonic manner with the decreasing temperature which is mainly due to the reduction of piezoelectric constant[9]. From the microscopic perspective, temperature variations will result in a significant nonlinear behavior in the material coefficients and hence will affect its overall performance. Piezoelectric parameters are decided by the piezoceramic material composition, dopants, and grain size, which are dependent on the magnitude of the temperature variations[10].

The warming structure for the piezoelectric stack was rarely studied and tested in the existing literatures. However, most researches are focused on the heat dissipation system for piezoelectric transformers whose maximum passing current and power capacity are limited by the temperature rise caused by heat generation, especially in the case of high output current for a long time[11-12]. Su et al.[13] proposed to add a thermal pad to the piezoelectric transformer to dissipate heat and build a corresponding heat transfer model, and then experimental results showed that the proposed techniques could increase by three times the output current of the piezoelectric transformer. The success of the heat dissipation system provides references for the design of a warming structure. Wang et al.[14] proposed an ultrasonic drill driven by the single crystal piezoelectric rings piezoelectric transducer and studied the resonant characteristics of the piezoelectric transducer at hyperthermal and cryogenic environments.

Recently, a few investigations have been carried out to warm the piezoelectric stack up in the cryogenic environment. After Balakrishna et al.[15-16] found that internal heating in the cryogenic wind tunnel did not work well for the piezoelectric stack, they redesigned a new heating system for the low-temperature tests, which was able to keep the piezoelectric damper device at room temperature when the ambient temperature was −150 ℃. However,

the implementation details and working principles of the heating system are not specified. This study has testified that it is necessary and feasible to use some heating methods to keep piezoelectric stacks well functional at workable temperatures.

In this paper, a convenient and effective warming structure is designed based on the operational characteristics of the piezoelectric stack and modeled by means of both one dimension and two dimensions' theoretical analysis. Analytical solutions for two-dimensional heat conduction and results from finite element analysis are compared to verify the feasibility of the proposed thermal insulating and heating structure.

1 Structural Design and Theoretical Analysis

1.1 Structural design

As an actuator, the piezoelectric stack is a good candidate for many applications, such as precision positioning, structural health monitoring, and active damping, because of its sizeable blocking force, high bandwidth, and relatively minor nonlinearity. As shown in Fig.1, piezoelectric stacks are installed at the rear transition of the cantilever sting, which are treated as actuators in the damping system. When the piezoelectric stack actuators are working, the output force from the tip of piezoelectric stacks would be exerted at the front end of the rear transition, and thus a counter-vibration moment would be generated to the supporting system.
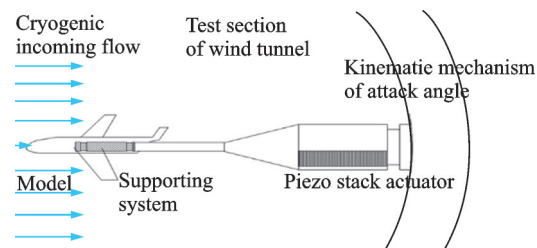
Fig.1 Example of piezo stack driving in the cryogenic environment

However, when operating in the cryogenic environment, the output displacement of piezoelectric stack actuators would be degraded as the tempera-

ture decreases. At the same time, compared to the encapsulated piezo stack actuator with the spherical hinge contact, the bare piezo stack actuator with plane contact is of the greater output performance because of the larger contact area, especially under critical stress conditions and for long time operations.

Thus, in this paper, we designed thermal insulation for the bare piezo stack actuator with the plane contact. Fig.2 depicts a schematic of the insulation and heating combined structure with the quadrangular prism shape. As can be seen, the heating film is attached to the outer surface of the piezoelectric stack, and then the outside of the heating film is wrapped with the heat insulation materials. At last the entire structure is installed in a metal cavity located in the cryogenic environment.
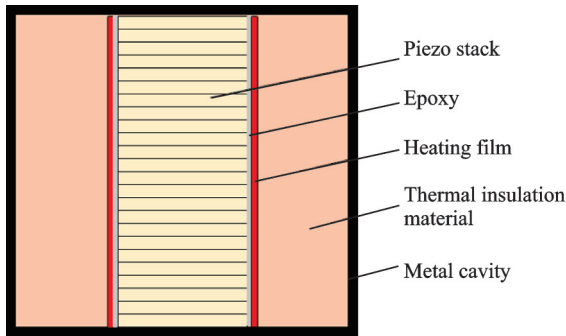
Fig.2   Schematic of the proposed piezo stack thermal insulating structure

1. 2   One-dimensional modeling and analysis

The objective of the thermally insulating structure is to maintain the temperature distribution of the piezoelectric stack at room temperature while in the cryogenic environment. If the steady-state temperature distribution of the piezoelectric stack could ideally stay around room temperature, the output performance of the piezoelectric stack would be the same as that at room temperature.

The piezoelectric stack is entirely wrapped by a heating film. As seen in Fig.3, the thermal insulation material layer can be regarded as adiabatic boundaries. Besides, the epoxy layer could also be neglected because the thickness of the epoxy is too small, and the specific thermal conductivity of epoxy is close to that of the piezoelectric stack. Thus, the heating film and the piezoelectric stack could be

regarded as the direct contact.

According to the energy conservation equation[17-21]

$$\phi_y + \mathrm{d}\phi_y = \phi_{y+\mathrm{d}y} + \Delta \tag{1}$$

where ϕ_y and $\phi_{y+\mathrm{d}y}$ are the heat transfer rate entering in and coming out of the control volume, respectively; $\mathrm{d}\phi_y$ represents the internal heat generation, and Δ the thermodynamic energy increment of the control volume. The heating film wrapped around the piezoelectric stack can be viewed as the internal heat generation in the one-dimensional analysis.
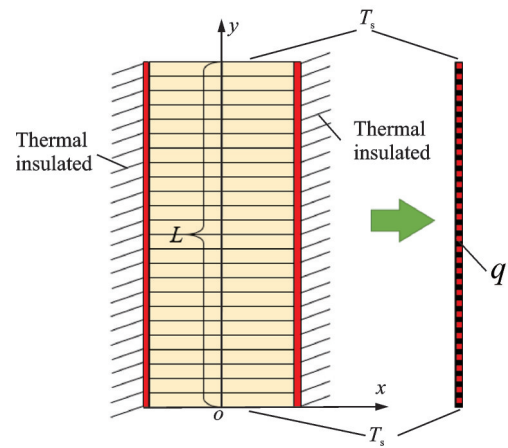
Fig.3   Schematic of the one-dimensional thermal problem

The corresponding definitions are

$$\phi_y = -kA\frac{\mathrm{d}T}{\mathrm{d}y} \tag{2}$$

$$\mathrm{d}\phi_y = q \cdot \mathrm{d}A_s \tag{3}$$

$$\phi_{y+\mathrm{d}y} = \phi_y + \frac{\mathrm{d}\phi_y}{\mathrm{d}y}\mathrm{d}y = \phi_y + \frac{\mathrm{d}}{\mathrm{d}y}\left(-kA\frac{\mathrm{d}T}{\mathrm{d}y}\right)\mathrm{d}y \tag{4}$$

$$\Delta = \rho c\dot{T}\mathrm{d}y \tag{5}$$

The boundary conditions of the two ends are

$$y = 0, T = T_s \tag{6}$$

$$y = L, T = T_s \tag{7}$$

where T_s and L are the outer temperature and the length of the piezoelectric stack, respectively.

When considering the steady-state heat conduction problems, the thermodynamic energy increment of the control volume Δ would always be zero. Thus

$$q \cdot \mathrm{d}A_s = \frac{\mathrm{d}}{\mathrm{d}y}\left(-kA\frac{\mathrm{d}T}{\mathrm{d}y}\right)\mathrm{d}y \tag{8}$$

Assuming the specific thermal conductivity k is the constant, Eq.(8) can be simplified as

$$q \cdot \mathrm{d}A_s = -kA \frac{\mathrm{d}^2 T}{\mathrm{d}y^2} \mathrm{d}y \qquad (9)$$

The perimeter of the heating film is P, then $\mathrm{d}A_s = P\mathrm{d}y$, thus Eq.(9) can be further simplified as

$$\frac{\mathrm{d}^2 T}{\mathrm{d}y^2} + \frac{\dot{\Phi}}{k} = 0 \qquad (10)$$

where $\dot{\Phi} = \dfrac{qP}{A}$. The solution of Eq.(10) is

$$T(y) = -\frac{\dot{\Phi}}{2k} y^2 + \frac{\dot{\Phi}L}{2k} y + T_s \qquad (11)$$

When the piezoelectric stack is driving in the cryogenic environment, the front and back ends of the piezoelectric stack would make direct contact with the metal structure, which bears the force output of the piezoelectric stack. The force transmission path is also the main heat transfer route of the piezoelectric stack. Therefore, the contact thermal resistance of the piezoelectric stack and metal structure should be taken into account.

Based on the concept of the thermal contact resistance per unit area R_c[22], the heat conduction formula through the thermal contact resistance is obtained as

$$Q = A_a \frac{T_s - T_a}{R_c} \qquad (12)$$

Usually, the geometry of the metal structure is complicated, so in our research, the temperature of the metal structure is assumed to be the ambient, temperature T_∞, as shown in Fig.4. This assumption is acceptable because the steady-state solution is only considered, and the specific thermal conductivity of the metal structure is much larger than that of the piezoelectric materials. Then the temperature T_s can be obtained as

$$T_s = \frac{QR_c}{A_a} + T_\infty \qquad (13)$$
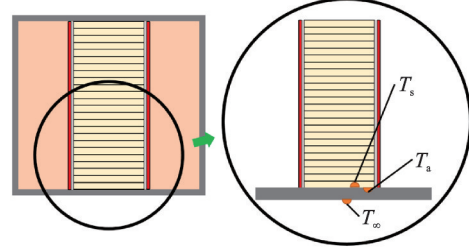
Fig.4   Schematic of the contact of piezo stack and housing structure

The relevant dimension and material parameters mentioned above are listed in Table 1.

Different heating power would lead to various temperature distributions of the piezoelectric stack actuator within the cryogenic environment. Fig.5 depicts the temperature distribution of the piezoelectric stack actuator subjected to the boundary temperature $-45\ ℃$. Several conclusions could be drawn as follows.

(1) The overall trend of the temperature distribution is that the middle of the piezo actuator gets the highest temperature while the temperature of the top and bottom ends is the lowest. Furthermore, the temperature distribution follows the quadratic function.

(2) The more heating power the heating film generates, the higher the maximum temperature of the piezoelectric stack actuator could reach.

(3) No matter how much the heating power is, the maximum temperature gradient is always located at the top and bottom ends of the piezoelectric stack actuator. The maximum temperature gradient is positively correlated with the heating power of the heating film.

Table 1   Relevant dimension and material parameters

Parameter	Description	Value
A_m/m^2	Area of the mechanical structure	3.2×10^{-3}
$k_m/(\mathrm{W}\cdot(\mathrm{m}\cdot\mathrm{K})^{-1})$	Thermal conductivity of the mechanical structure	10
$k_p/(\mathrm{W}\cdot(\mathrm{m}\cdot\mathrm{K})^{-1})$	Thermal conductivity of the piezoelectric stack	1.5
l_m/m	Thickness of the mechanical structure	1.6×10^{-2}
l_p/m	Length of the piezoelectric stack	1.8×10^{-2}
Q/W	Rated power of the heating film	10
r_m/m	Radius of the mechanical structure	3.2×10^{-2}
w_p/m	Width of the piezoelectric stack	1.4×10^{-2}
d_p/m	Depth of the piezoelectric stack	1.4×10^{-2}
$R_c/(\mathrm{m}^2\cdot\mathrm{K}\cdot\mathrm{W}^{-1})$	Thermal contact resistance per unit area	5.8×10^{-4}
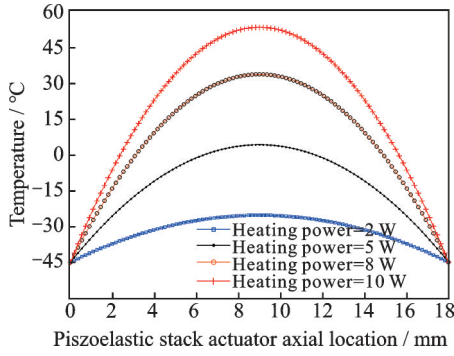
Fig.5   Temperature distributions along the axial direction with different heating power

1.3   Two-dimensional modeling and analysis

The two-dimensional heat conduction problem of the piezoelectric stack is shown in Fig.6. The stack is symmetrically distributed around the y axis, and the heat flux q generated by heating film is given along $x=a$ boundary. In order to obtain a single nonhomogeneous boundary condition, variable $\theta = T - T_s$ is introduced, where T_s is the temperature at the bottom end of the piezoelectric stack ($y=0$). Mathematically, the problem is formulated as[17-21]

$$\frac{\partial^2 \theta}{\partial x^2} + \frac{\partial^2 \theta}{\partial y^2} = 0 \tag{14}$$

The corresponding boundary conditions are

$$x = 0 \quad \frac{\partial \theta}{\partial x} = 0 \tag{15}$$

$$x = a \quad -k_p \frac{\partial \theta}{\partial x} = q \tag{16}$$

$$y = 0 \quad \theta = 0 \tag{17}$$

$$y = b \quad \frac{\partial \theta}{\partial y} = 0 \tag{18}$$
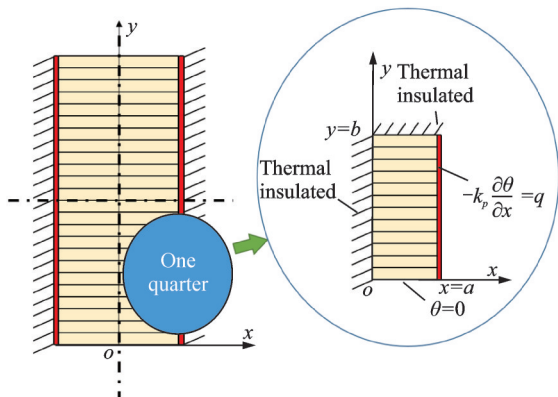
Fig.6   Schematic of the integral heating problem

The heating film in the two-dimensional analysis is treated as the boundary flux, which is quite different from the one-dimensional analysis.

The steady-state solution of this two-dimensional heat conduction problem[18] could be obtained by the separation of variables method. First, the temperature distribution function is assumed to be the product of the contained independent variable function.

$$\theta(x,y) = X(x)Y(y) \tag{19}$$

Substituting Eq.(19) into Eq.(14), we get

$$-\frac{X''(x)}{X(x)} = \frac{Y''(y)}{Y(y)} \tag{20}$$

The left part of Eq.(20) is the function of variable x, which is different from the right part, so Eq.(20) can only exist if both portions are equal to a constant.

Let the constant be λ, thus two ordinary differential equations(ODEs) are obtained as

$$X''(x) + \lambda X(x) = 0 \tag{21}$$

$$Y''(y) - \lambda Y(y) = 0 \tag{22}$$

The corresponding general solutions of these two ODEs are

$$X(x) = C_1 e^{\sqrt{-\lambda}\, x} + C_2 e^{-\sqrt{-\lambda}\, x} \tag{23}$$

$$Y(y) = C_3 \cos(\sqrt{-\lambda}\, y) + C_4 \sin(\sqrt{-\lambda}\, y) \tag{24}$$

where the undetermined coefficients (C_1, C_2, C_3, C_4) are decided by boundary conditions.

By utilizing the boundary conditions, λ would be a negative number.

Thus assume

$$\lambda = -\beta^2 \tag{25}$$

where β is a non-zero real number, and the general solutions could be rewritten as

$$X(x) = A \sinh(\beta x) + B \cosh(\beta x) \tag{26}$$

$$Y(y) = C_3 \cos(\beta y) + C_4 \sin(\beta y) \tag{27}$$

where $A = C_1 - C_2, B = C_1 + C_2$.

From Eqs.(15) and (17), we get

$$C_3 = 0 \tag{28}$$

$$A = 0 \tag{29}$$

The solution could be simplified as

$$\theta(x,y) = D \cosh(\beta x) \sin(\beta y) \tag{30}$$

where $D = BC_4$.

From Eq.(18), we could further get

$$\beta = \frac{2n-1}{2b}\pi \quad n = 1,2,\cdots,\infty \tag{31}$$

The analytical solution is now

$$\theta(x,y) = \sum_{n=1}^{\infty} D_n \cosh\left(\frac{2n-1}{2b}\pi x\right) \sin\left(\frac{2n-1}{2b}\pi y\right) \tag{32}$$

From Eq.(16), we get

$$k \frac{\partial \theta}{\partial x}\bigg|_{x=a} = k_p \sum_{n=1}^{\infty} \frac{2n-1}{2b} \pi D_n \sinh\left(\frac{2n-1}{2b}\pi a\right)\sin\left(\frac{2n-1}{2b}\pi y\right) = q \tag{33}$$

Let $E_n = \frac{2n-1}{2b}\pi D_n \sinh\left(\frac{2n-1}{2b}\pi a\right)$, Eq.(33) could be rewritten as

$$\sum_{n=1}^{\infty} E_n \sin\left(\frac{2n-1}{2b}\pi y\right) = \frac{q}{k_p} \tag{34}$$

Because q/k_p is the function defined in the interval of $[0, b]$,

$$E_n = \frac{2}{b}\int_0^b \frac{q}{k_p}\sinh\left(\frac{2n-1}{2b}\pi y\right)\mathrm{d}y \tag{35}$$

So the coefficient of Eq.(32) is obtained as

$$D_n = \frac{2b}{(2n-1)\pi}\frac{2q}{bk_p}\frac{1}{\sinh\left(\frac{2n-1}{2b}\pi a\right)}\int_0^b \frac{q}{k_p}\sinh\left(\frac{2n-1}{2b}\pi y\right)\mathrm{d}y \tag{36}$$

The solution to this problem is

$$\theta(x,y) = \frac{4q}{\pi k_p}\sum_{n=1}^{\infty}\frac{\int_0^b \frac{q}{k_p}\sinh\left(\frac{2n-1}{2b}\pi y\right)\mathrm{d}y}{(2n-1)\sinh\left(\frac{2n-1}{2b}\pi a\right)}\cosh\left[\frac{(2n-1)\pi}{2b}x\right]\sin\left[\frac{(2n-1)\pi}{2b}y\right] \tag{37}$$

where $n = 1, 2, \cdots$. According to the definition of θ, the final temperature distribution function $T(x,y)$ should be corrected with the boundary temperature T_s. Therefore, the temperature distribution function of the piezoelectric stack $T(x,y)$ can be obtained as

$$T(x,y) = \theta(x,y) + T_s \tag{38}$$

Since the bottom of the piezoelectric stack is also covered with a layer of thin heating film, its temperature can be regarded as uniform and equal to the bottom temperature of the stack, and the heat is transferred to the external environment through the mechanical structure. Due to the thermal contact resistance on the interface between the bottom of the piezoelectric stack and the housing structure, the temperature of the housing structure T_a is lower than T_s. Based on the definition of thermal contact resistance per unit area $R_c^{[22]}$, the heat conduction formula could be given by

$$Q = A_a\frac{T_s - T_a}{R_c} \tag{39}$$

In terms of the heat conduction from the housing metal structure to the external environment, which could be considered as the one-dimensional steady-state conduction through the plane wall[18], the formula is obtained as

$$T_a \approx T_\infty \tag{40}$$

where T_∞ is the reachable lowest ambient temperature. Combining Eqs.(39, 40), the boundary temperature of the piezoelectric stack is

$$T_s = \frac{QR_c}{A_a} + T_\infty \tag{41}$$

The calculation results of the temperature distribution in the piezoelectric stack with various heating power are illustrated in Fig.7. From Fig.7, several observations could also be obtained as follows.

(1) The maximum temperature is located at the outer surface of the middle part of the piezoelectric stack actuator. Furthermore, the more the heating power is, the larger the maximum temperature of the piezoelectric stack actuator would be.

(2) The temperature distribution of the piezoelectric stack actuator gradually decreases from the middle part to the top and bottom ends with the same x coordinate.

(3) Similarly, the temperature distribution with the same y coordinate is enhanced from the inner to the outer.

Fig.8 depicts the comparison between the one-dimensional analysis and two-dimensional analysis. It can be obviously seen that temperature increments of both one-dimensional and two-dimensional results increase from the boundary to the central plane. The average temperature increments of 2D is lower than that of the 1D in the same position, and the difference becomes larger with the increase of axial location. One possible reason is that the thermal load is applied differently. In one-dimensional analysis, the thermal load is applied as the internal heat source, while in two-dimensional analysis, the

(a) Heating power=2 W

(b) Heating power= 5 W

(c) Heating power=8 W
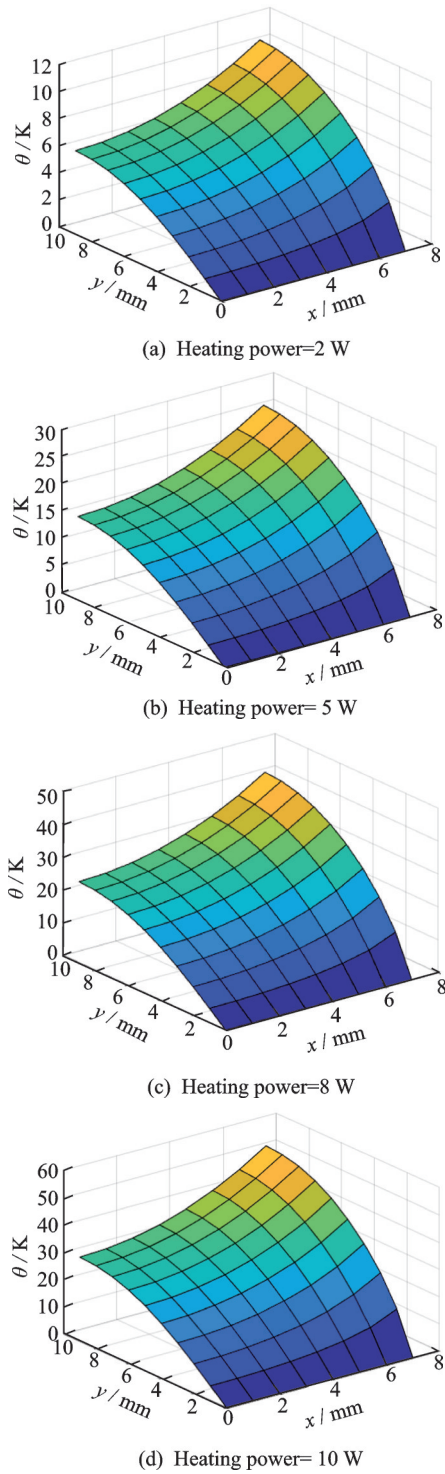
(d) Heating power= 10 W

Fig.7   Temperature distribution of the piezoelectric stack with various heating power

thermal load is applied as a boundary condition.

As a characterization of temperature uniformity, the standard deviation increases rapidly with the axial position, and then the standard deviation remains almost unchanged. This means that the temperature difference in the middle of the stack is the largest. The possible reason for this phenomenon is

that the aspect ratio of the piezoelectric stack is not as large as expected. However, these results give us a theoretical reference for the design of piezoelectric stack heating and insulation.

(a) Heating power=2 W

(b) Heating power= 5 W

(c) Heating power=8 W

(d) Heating power= 10 W
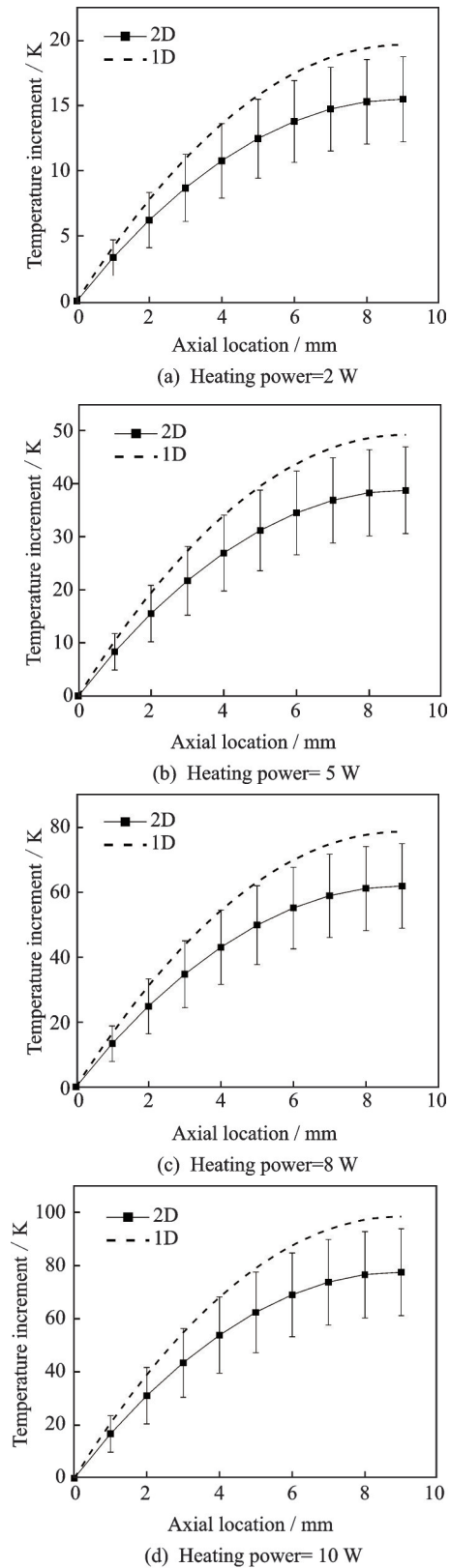
Fig.8   Comparison between one- and two-dimensional results

2 Finite Element Validation

The finite element analysis is also carried out to verify the theoretical results in the previous section. According to the characteristics of the warming structure, the finite element model is built through the COMSOL Multiphysics software, as shown in Fig.9. A thin air layer as the medium for heat transfer of the thermal contact in practice is set between the piezoelectric stack and the housing structure. By considering the accuracies of machining and installation of the structures, the air layer between the bottom packaging housing and mechanical structure is set as 0.2 mm in the model. Therefore, the thermal contact resistance can be simulated, and the reliability of the results also can be improved. The heating power of the heating film is set to 5 W.
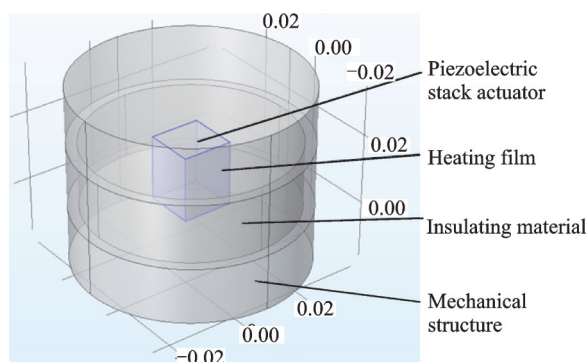
Fig.9 Finite element model

Table 2 provides the material properties used in the simulation. The boundary conditions are set consistently with the theoretical model. A tetrahedral mesh is used for calculation. The simulation of the temperature field is carried out on the finite element model.

Table 2 Material properties of finite element model

Structure	Material	Density/ $(kg \cdot m^{-3})$	Thermal conductivity/ $(W \cdot (m \cdot K)^{-1})$	Thermal expansion coefficient/ $10^{-6} \cdot (\text{℃})^{-1}$	Heat capacity/ $(J \cdot (kg \cdot K)^{-1})$
Piezoelectric stack	Piezoelectric ceramic	7 750	1.5	2	420
Heating film	Polyimide	1 400	0.15	18	109
Insulation material	Aerogel	180	0.007	—	502
Mechanical structure	Invar	8 100	10	1.5	515

The finite element results of the temperature distribution in the entire structure and the piezoelectric stack are shown in Fig.10.

Fig.11 shows the comparison of the temperature distribution between the theoretical solution and simulation results at the symmetry axis of the piezoelectric stack. Compared with Fig.8, the results of the two-dimensional analysis in Fig.11 are corrected by the equivalent heating method. It is apparent that the FEM results are well consistent with the two-dimensional analysis from 0 to 9 mm, and a slight deviation of only 0.91 K is observed at 9 mm.

Another obvious result that should be paid attention to is that the difference between the standard deviation of two-dimensional analysis and the standard deviation of FEM gradually increases from the edge to the middle in the axial direction. This indicates that the uniformity of FEM results is higher than that of two-dimensional analysis. This can be explained by the difference between the two heating methods. In the two-dimensional analysis, the heating in other directions is equivalently replaced by the heating boundary condition, while in the FEM analysis, the heat flow is transmitted from the periphery of the piezoelectric stack to the interior.

The above findings indicate that both theoretical and finite element analyses have reliability and validity. Consequently, the simulation results further verify that the warming structure is able to keep the piezoelectric stack at normal temperature with moderate temperature standard deviations.

(a) Temperature distribution of the whole piezo body

(b) Temperature distribution of the middle section
of the piezoelectric stack
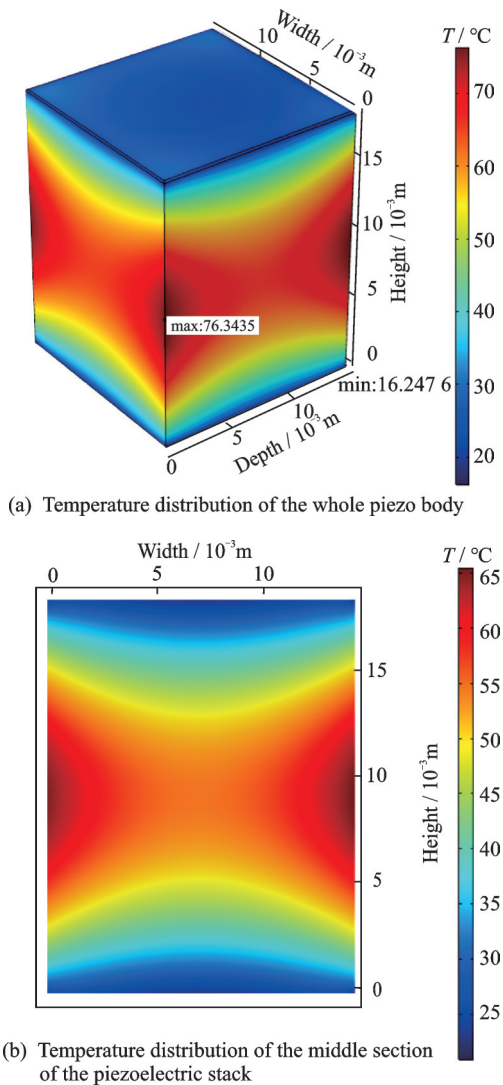
Fig.10　Finite element simulation results
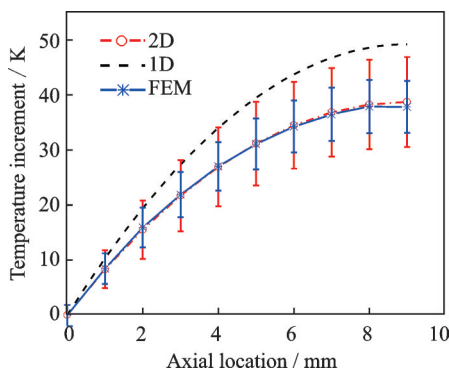
Fig.11　Comparison between theoretical and simulation results

3　Conclusions

This paper proposes a heating and insulation structure for keeping the piezoelectric stack actuator functionally working well in the cryogenic environment. The warming structure is modeled and analyzed with one- and two-dimensional theoretical anal-

yses. The one-dimensional analysis shows that the temperature with heating film working follows the quadratic distribution in the axial direction. In two-dimensional theoretical analysis, the temperature distribution of the piezoelectric stack actuator gradually decreases from the middle part to the top and bottom ends with the same x coordinate. The temperature distribution with the same y coordinate is enhanced from the inner part to the outer part. The results of the theoretical analysis are compared with the finite element simulation analysis. The finite element method results show a good consistency with the two-dimensional theoretical results from 0 to 9 mm. A slight deviation of only 0.91 K is observed at 9 mm, indicating that the proposed scheme is of the potential for preventing the piezoelectric stack from being damaged in the cryogenic environment. The advantage of the proposed theoretical solution is that the temperature distribution of the piezoelectric stack actuator could be evaluated quickly and the tendency of the temperature distribution could also be obtained with respect to the heating power. At last the experiment about the temperature distribution under different heating power would be carried out in the future work.

References

[1]　FEHREN H, GNAUERT U, WIMMEL R, et al. Validation testing with the active damping system in the European Transonic Wind tunnel[C]//Proceedings of the 39th AIAA Aerospace Sciences Meeting and Exhibit. [S.l.]: AIAA, 2001:610.

[2]　BALAKRISHNA S, HOULDEN H, BUTLER D, et al. Development of a wind tunnel active vibration reduction system[C]//Proceedings of AIAA Aerospace Sciences Meeting & Exhibit. [S.l.]: AIAA, 2007:961.

[3]　ZHANG L, DAI Y, SHEN X, et al. Research on an active pitching damper for transonic wind tunnel tests[J]. Aerospace Science and Technology, 2019, 94:105364.

[4]　DAI Y, ZHANG L, ZHAO Z, et al. Wind-tunnel evaluation for an active sting damper using multimodal neural networks[J]. AIAA Journal, 2020, 58(4): 1-10.

[5]　SHEN X, LI Y, LIANG L, et al. Self-sensing test method for the temperature of piezoelectric stacks[J]. Transactions of Nanjing University of Aeronautics and

Astronautics, 2019,36(1):109-118.

[6]　SHERRIT S, DAPINO M J, OUNAIES Z, et al. Multilayer piezoelectric stack actuator characterization[J]. Proceedings of SPIE—The International Society for Optical Engineering, 2008, 6929:692909.

[7]　SHERRIT S, BAO X, JONES C M, et al. Piezoelectric multilayer actuator life test[J]. IEEE Transactions on Ultrasonics, Ferroelectrics, and Frequency Control, 2011, 58(4):820-828.

[8]　TAYLOR R P, NELLIS G F, KLEIN S A, et al. Measurements of the material properties of a laminated piezoelectric stack at cryogenic temperatures[C]//Proceedings of AIP Conference. [S.l.]: American Institute of Physics, 2006.

[9]　SHINDO Y, NANTA F, SASAKURA T. Cryogenic electromechanical behavior of multilayer piezo-actuators for fuel injector applications[J]. Journal of Applied Physics, 2011, 110(8):84510.

[10]　SABAT R G, MUKHERJEE B K, REN W, et al. Temperature dependence of the complete material coefficients matrix of soft and hard doped piezoelectric lead zirconate titanate ceramics[J]. Journal of Applied Physics, 2007, 101(6):121-126.

[11]　SHAO W W, CHEN L J, PAN C L, et al. Power density of piezoelectric transformers improved using a contact heat transfer structure[J]. IEEE Transactions on Ultrasonics, Ferroelectrics, and Frequency Control, 2012, 59(1):73-81.

[12]　LI P Y, HAN Z L, SHAO W W, et al. A study on the equivalent circuit of longitudinal vibration piezoelectric transformers with contacted heat transfer device[C]//Proceedings of 2016 Symposium on Piezoelectricity, Acoustic Waves, and Device Applications (SPAWDA). [S.l.]: IEEE, 2016:147-148.

[13]　SU Y H, LIU Y P, VASIC D, et al. Power enhancement of piezoelectric transformers by adding heat transfer equipment[J]. IEEE Transactions on Ultrasonics, Ferroelectrics, and Frequency Control, 2012, 59(10):2129-2136.

[14]　WANG T, QUAN Q, TANG D, et al. Effect of hyperthermal cryogenic environments on the performance of piezoelectric transducer[J]. Applied Thermal Engineering, 2021, 193:116725.

[15]　BALAKRISHNA S, BUTLER D, ACHESON M, et al. Design and performance of an active sting damper for the NASA common research model[C]//Proceedings of AIAA Aerospace Sciences Meeting Including the New Horizons Forum & Aerospace Exposition.[S.l.]: AIAA, 2013.

[16]　RIVERS M B, BALAKRISHNA S. NASA common research model test envelope extension with active sting damping at NTF[C]//Proceedings of American Institute of Aeronautics and Astronautics 32nd AIAA Applied Aerodynamics Conference. [S.l.]: AIAA, 2014.

[17]　INCROPERA F P, DEWITT D P. Fundamentals of heat and mass transfer edition [M]. 4th ed. [S.l.]: Wiley, 1996.

[18]　ZHANG Jingzhou. Advanced heat transfer[M].2nd ed Beijing: Science Publishing, 2015. (in Chinese)

[19]　LI Feiran, LI Jun, JIANG Yanlong, et al. Temperature field of plate-fin heat exchanger based on joint simulation[J]. Journal of Nanjing University of Aeronautics & Astronautics, 2021, 53(2):313-319. (in Chinese)

[20]　ZHANG Jingzhou, CHANG Haiping. Heat transfer [M].2nd ed. Beijing: Science Publishing, 2009: 33-67. (in Chinese)

[21]　TAO Wenquan. Heat transfer[M]. Xi'an: Northwestern Polytechnical University Publishing, 2006:39-54. (in Chinese)

[22]　INCROPERA F P, DEWITT D P. Fundamentals of heat and mass transfer[M]. Beijing: Chemical Industry Publishing,2007:67-81.

Authors　　Mr. **ZHANG Lei** received his B. S. degree in aircraft design and engineering from Nanjing University of Aeronautics and Astronautics in 2015, and joined the State Key Laboratory of Mechanics and Control of Mechanical Structures as a Ph.D. candidate. His main research field is active vibration control and smart structures.

Prof. **SHEN Xing** received the Ph.D. degree from Nanjing University of Aeronautics and Astronautics in 2003. He is now a professor at Nanjing University of Aeronautics and Astronautics. His research is focused on aeronautical smart structure, including design and test of the piezoelectric ceramics, piezoelectric sensors and actuators and relative research in the smart material structure.

Author contributions　　Mr. **ZHANG Lei** designed the scheme and wrote the manuscript. Ms. **XIAO Yan** contributed to the background and discussion of the results. Mr. **JIANG Yongping** contributed to the improvement of the model and

低温环境下压电叠堆隔热加热方案设计与分析

张　磊[1]，肖　艳[2]，姜永平[3]，陈明绚[4]，沈　星[1]

（1.南京航空航天大学机械结构力学及控制国家重点实验室,南京 210016,中国；2.上海卫星工程研究所,上海 200240,中国；3.中国飞机强度研究所,西安 710065,中国；4.南京晨光集团有限责任公司,南京 210006,中国）

摘要：在低温风洞试验中,通常采用压电叠堆实现悬臂支杆的振动控制。然而,随着温度的降低,压电叠堆的最大自由位移和最大输出力将显著降低。本文提出了一种方便有效的压电堆加热结构方案,当环境温度下降时,该结构可以使压电堆在工作温度下工作。首先,采用聚酰亚胺加热膜包裹压电叠堆,然后在外部用气凝胶材料包裹以实现隔热目的。压电叠堆的两端与有效载荷结构直接接触。接着,对压电叠堆的热传导问题进行了一维和二维理论分析。最后,采用有限元方法验证了理论分析的结果。有限元计算结果与二维理论结果具有良好的一致性,仅观察到 0.91 K 的微小偏差,显示了本方案在低温下保护压电叠堆的潜力。

关键词：压电叠堆；低温环境；加热结构；一维热传导；二维热传导